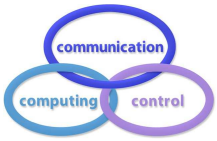
INTERNATIONAL JOURNAL OF COMPUTERS COMMUNICATIONS & CONTROL
Online ISSN 1841-9844, ISSN-L 1841-9836, Volume: 21, Issue: 6, Month: December, Year: 2026
Article Number: 7750, https://doi.org/10.15837/ijccc.2026.6.7750



CCC Publications



Electromagnetic Interference Robustness and Synchro-nization Scalability in Wireless Battery Management Systems for Electric Vehicles

Attila Simo, Simona Dzitac, Bogdan-Constantin Neagu, Horea Oros

Attila Simo
Faculty of Electrical and Power Engineering
Politehnica University of Timisoara, Romania
attila.simo@upt.ro

Bogdan-Constantin Neagu
Faculty of Electrical Engineering
"Gheorghe Asachi" Technical University Iasi, Romania
bogdan-constantin.neagu@academic.tuiasi.ro

Simona Dzitac
Department of Energy Engineering
University of Oradea, Romania
Corresponding author: simona@dzitac.ro

Horea Oros
Department of Mathematics and Computer Science
University of Oradea, Romania
horos@uoradea.ro

Abstract

The transition toward wireless battery management systems (wBMS) promises a substantial reduction in wiring complexity and mass for electric-vehicle (EV) battery packs, yet automotive-grade deployment is still constrained by two interlocking barriers: electromagnetic-interference (EMI) robustness and network-synchronization scalability. Building directly on a companion study that experimentally validated an eight-node chip-on-cell wireless cell-monitoring-unit (CMU) network based on the Dukosi DK8x02 platform, this paper develops and calibrates an analytical framework that projects how that demonstrated architecture, together with a representative time-division-multiple-access (TDMA) alternative, behaves as pack size grows toward automotive-relevant node counts. A near-field/far-field link-budget model quantifies the link-margin erosion produced by traction-inverter switching noise for the near-field-communication (NFC) and Bluetooth Low Energy (BLE) physical layers; a bit-error-rate model translates that margin into packet-failure probability; and a discrete time-slot model propagates packet failure into network-formation latency and pack-level current draw, calibrated against the 0.09 A per-CMU current measured in the companion demonstrator and against published automotive wireless-BMS benchmarks. The results show that polling-based NFC networks scale linearly but with roughly an order-of-magnitude higher latency than TDMA/BLE architectures, that electro-magnetic aggression measurably yet non-catastrophically inflates both latency and current draw once adequate link margin and frequency-hopping are present, and that only the TDMA/BLE branch is presently positioned to meet ASIL-D-class functional-safety timing budgets under ISO 26262. The paper closes with concrete design guidance on shielding placement, slot-time budgeting, and standards alignment for next-generation automotive wBMS.

Keywords: Wireless Battery Management System; Electromagnetic Interference; Time Synchronization; Bit Error Rate; ISO 26262; ASIL; Chip-on-Cell Monitoring; Elec-tric Vehicles.

1 Introduction

Electric-vehicle battery packs are managed by increasingly sophisticated battery management systems (BMS) that estimate state of charge and health, balance cells, and guard against thermal and electrical faults. Conventional architectures rely on a dense sense-wire harness linking every cell-monitoring circuit to a central controller, adding mass, assembly cost, and long-term reliability risk as connectors age [8], [15]. Wireless battery management systems (wBMS) replace most of that harness with radio or near-field links between cell supervisory circuits (CSCs) and the battery management controller (BMC), and have moved from laboratory curiosity to commercial reality: General Motors' Ultium platform fields a proprietary 2.4 GHz encrypted link developed with Analog Devices [21], and Texas Instruments has obtained an independent TÜV SÜD ASIL-D assessment for its own wireless BMS protocol [22].

In a companion study we reported the design and experimental validation of a chip-on-cell wBMS demonstrator built around the Dukosi DK8x02 evaluation kit, with Vitesco Technologies Engineering Romania [1]. That work networked eight cell-monitoring units (CMUs) over a near-field-communication (NFC) link, through both a USB-and-GUI configuration and a direct SPI integration with an automotive-grade BMC, and measured an average current draw of 0.09 A per CMU. The demonstrator confirmed that chip-on-cell wireless monitoring is achievable with commercial hardware, but left open the two questions that determine series-production readiness: how robust is the link to a traction inverter's electromagnetic environment, and how does synchronization scale once eight CMUs become the forty-eight to ninety-six cells of a full pack? The present paper answers both analytically, using the companion demonstrator as a calibration point rather than repeating it physically.

1.1 Related Work

Reviews of wBMS technology consistently flag electromagnetic interference and real-time synchronization as first-order barriers to automotive qualification, even without quantifying them. Cao et al. [2] survey BLE, ZigBee, Wi-Fi, NFC and UWB and note that BLEs frequency-hopping and Gaussian frequency-shift keying give it comparatively good noise resilience, a property exploited directly in Section 2.2. Samanta and Williamson [3] reach a similar conclusion, favoring BLE and ZigBee for low-power EV use while flagging EMI robustness as unresolved. Na et al. [4] built and tested a Bluetooth-based wBMS prototype on real EV modules, underlining the need for tight hardware–software co-design to keep the network synchronized — formalized here as a discrete time-slot model in Section 2.3.

Electromagnetic coupling has begun to receive dedicated experimental attention outside the automo-tive-BMS literature narrowly defined. Je Lee et al. [17] characterized RF interference on a Bluetooth-based wBMS in a high-congestion 2.4 GHz environment and found that shielding only partially recovers the degradation, consistent with the shielding-loss term adopted in Section 3.1. Riurean and Rus [16] argue that conventional RF wBMS links remain fundamentally EMI-limited and propose optical communication as an EMI-immune alternative — an implicit acknowledgement that the EMI question addressed here for RF links is still open for the approach that dominates commercial deployment. Basic et al. [5], Shell et al. [6], and Lee et al. [7] confirm that security and basic link reliability both remain active concerns.

On the safety-standards side, Prüfling et al. [18] and John and Kumar [19] discuss functional-safety practice and ISO 26262 compliance for wireless BMS. Texas Instruments' documentation for its CC2662R-Q1 chipset [22] is, to our knowledge, the most complete public account of what an ASIL-D-relevant wireless communication layer must deliver: packet error rate below 10^{-7}, availability above 99.999%, network restart within 300 ms, and per-node latency below 2 ms for up to 100 nodes - figures used throughout Section 3 as an external benchmark. Murlidharan et al. [9] extend the discussion into cybersecurity, revisited briefly in Section 4. The broader literature — Gabbar et al. [8], Ghazali et al. [10], Kumar [11], Mulpuri et al. [12], Ren et al. [13], and Balasingam et al. [14] — continues to mature algorithms and architectures generally, but none addresses the EMI/synchronization coupling that is this paper's focus.

1.2 Research Gaps

1. Electromagnetic-interference robustness is treated qualitatively throughout the wBMS literature [2], [3], [8], [16]; no published quantitative link-budget or bit-error-rate model exists for the near-field and 2.4 GHz physical layers used at cell level under realistic inverter switching noise.

2. Synchronization is documented only as a protocol-agnostic generality or a single manufacturer's specification [22], [21]; no comparative model spans polling-based (NFC/RFID) and TDMA-based (BLE) architectures as node count scales toward the forty-eight to ninety-six cells of a production pack.

3. No study calibrates such a scaling model against an independently reported, physically demonstrated chip-on-cell baseline: simulation-only work lacks empirical anchoring, and prototype-only work — including our own companion study [1] — lacks the analytical apparatus to project beyond the tested configuration.

4. ISO 26262 alignment is discussed narratively [19], [20] but rarely connected quantitatively to the communication-layer error and latency budgets that determine ASIL feasibility.

5. The coupling between EMI-induced retransmissions and pack-level power draw has not, to our knowledge, been modeled quantitatively for automotive wBMS.

1.3 Contribution and Novelty of This Work

This paper addresses these gaps through an integrated analytical study that: (i) derives closed-form link-budget and bit-error-rate models for the NFC and BLE physical layers under two automotive EMI severity scenarios (3.1); (ii) propagates the resulting packet-failure probabilities through a discrete time-slot synchronization model to project network-formation latency from the eight-CMU configuration validated in [1] up to ninety-six CMUs, for a polling-based and a TDMA-based architecture (3.2); (iii) calibrates a power-budget projection against the 0.09 A per-CMU current measured in that demonstrator (3.3); (iv) benchmarks both projections against the only publicly documented ASIL-D-assessed commercial wBMS layer [22]; and (v) maps the results onto ISO 26262 ASIL allocation as design guidance. The novelty lies in the quantitative bridge built between a real, previously reported data point and a scalable analytical model — absent, on the evidence of Section 1.1, from the current literature.

2 Background: Electromagnetic Coupling and Synchronization Fundamentals

Two physical mechanisms decide whether a wireless CSC network can replace a wiring harness: how much of the transmitted signal survives the pack's electromagnetic environment, and how quickly the resulting bits assemble into a synchronized network. This section develops the models quantified in Section 3.

2.1 Electromagnetic Environment of an EV Battery Pack

Traction inverters switch hundreds of amperes at 10–20 kHz fundamentals, using silicon-carbide or IGBT devices whose fast switching edges generate broadband harmonics extending into the VHF/low-UHF range relevant to both the 13.56 MHz NFC band and the 2.4 GHz ISM band [17]. This noise reaches a wireless CSC network through two paths, sketched in Fig. 1: conducted emissions along the wiring harness, and radiated emissions coupling directly into CMU antennas or NFC loops. The pack's metal enclosure attenuates the radiated path but does not eliminate it, as confirmed experimentally for a Bluetooth-based wBMS by Je Lee et al. [17]. Automotive EMC limits for this environment are set by CISPR 25 [26], used qualitatively here to bound the noise-floor increase adopted in Section 3.1.

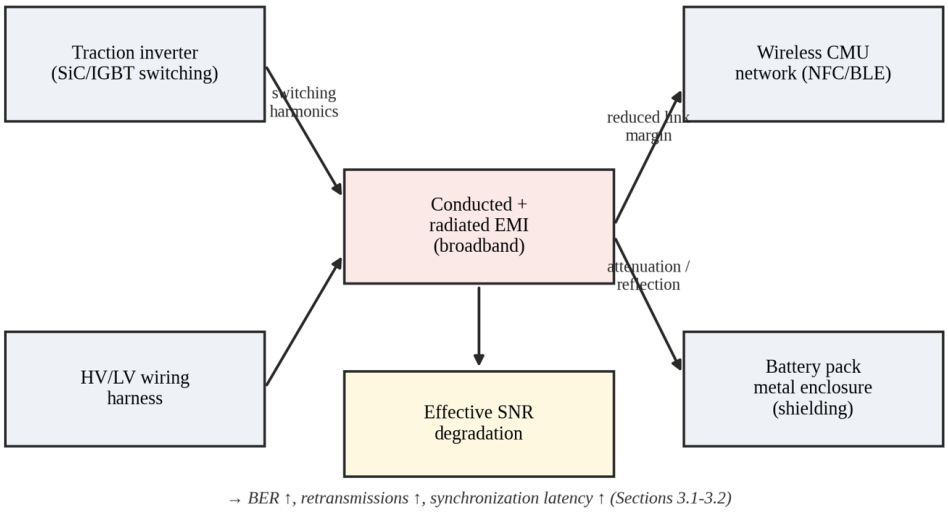


Figure 1: Conducted and radiated EMI coupling paths from the traction inverter into a wireless CMU network.

2.2 Physical-Layer Susceptibility: Near-Field versus Far-Field Coupling

The companion demonstrator's chip-on-cell CMUs communicate by near-field coupling at 13.56 MHz, in the manner of an ISO 15693 vicinity-card link [24]. Near-field magnetic coupling between small loop antennas falls off approximately as the sixth power of separation distance [23], so link margin erodes at roughly 60 dB per decade — far steeper than a conventional radio link. BLE, by contrast, operates as a far-field radio governed by the Friis equation, with free-space path loss growing at 20 dB per decade, and further employs frequency-hopping spread spectrum and Gaussian frequency-shift keying to resist the narrowband interference an inverter's switching harmonics can produce [2]. These contrasting susceptibility profiles underpin the link-margin model solved in Section 3.1.

2.3 Synchronization Architectures and Functional-Safety Timing Budgets

Two medium-access families are relevant here. Sequential anti-collision polling, characteristic of NFC/RFID inventory rounds, addresses one CMU at a time and is implicit in the companion demonstrator's USB-and-GUI and SPI configurations [1], [23]. Time-division multiple access (TDMA) allocates each node a fixed slot within a repeating superframe, and is the architecture behind both GM's Ultium wBMS [21] and TI's ASIL-D-assessed protocol, which combines TDMA with deterministic modulation to guarantee sub-2 ms per-node latency for up to 100 nodes [22]; TDMA scheduling is now considered standard practice for wireless CMU networks generally [21]. ISO 26262 does not require the wireless link itself to reach the target ASIL: TI's safety concept instead treats the link as a 'black channel' wrapped in a safety layer that independently bounds communication-error response time [19], [20], [22] — precisely the quantity Section 3.2 projects as a function of pack size and EMI severity.

3 Results and Discussion

This section presents the calibrated analytical results in three steps: a link-budget and bit-error-rate analysis of the two physical layers (3.1), a synchronization-latency projection that uses those results to scale the companion demonstrator's eight-CMU network toward full-pack node counts (3.2), and a power-budget projection together with a comparative, standards-oriented discussion (3.3).

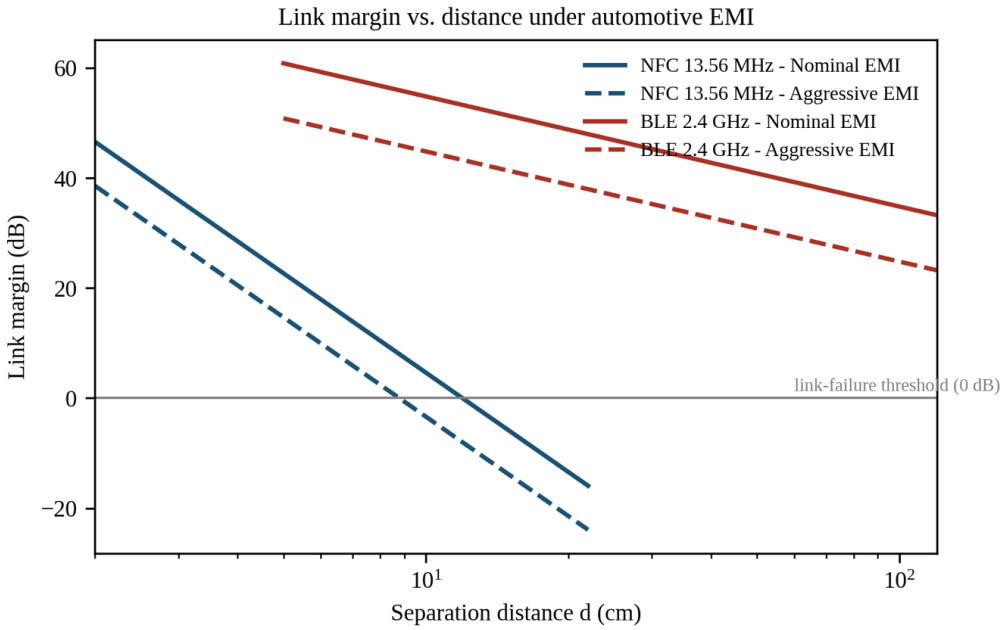


Figure 2: Link margin vs. separation distance for NFC and BLE physical layers under nominal and aggressive automotive EMI.

3.1 Link-Budget and Bit-Error-Rate Analysis under Automotive EMI

Link margin for the near-field NFC channel is modeled as $M_NFC(d) = M0 - 60 \cdot log_{10}(d/d0)$, with reference margin $M0 = 42$ dB at $d0 = 3cm$, typical of a chip-on-cell antenna mounted on the cell tab. Link margin for BLE follows the free-space path-loss form of the Friis equation,

$$FSPL(d) = 20 \cdot log_{10}(d) + 20 \cdot log_{10}(f) + 20 \cdot log_{10}(4\pi/c) \tag{1}$$

evaluated at $f = 2.44\ GHz$ with 0 dBm transmit power and $-95\ dBm$ receiver sensitivity typical of a BLE5 radio [22], reduced by a further 12 dB for enclosure attenuation. Fig. **??** plots both margins under nominal EMI (an inverter within CISPR 25 limits [26]) and aggressive EMI (degraded shielding or a fault raising the noise floor by $6 - 14\ dB$). Under nominal EMI, NFC retains positive margin to roughly 13 cm and BLE well beyond one metre; aggressive EMI contracts both distances — quantitatively supporting the antenna-placement caution our companion study could only state descriptively [1].

Translating margin into bit-error rate requires a modulation-specific model. For the noncoherent ASK used by ISO 15693-class NFC links, and the noncoherent GFSK used by BLE, the standard forms are

$$BER_ASK(\gamma) = 0.5 \cdot exp(-\gamma/4), BER_FSK(\gamma) = 0.5 \cdot exp(-\gamma/2) \tag{2}$$

where γ is linear SNR [25]. Fig. 3 plots both curves against SNR, with the 10^{-5} telemetry target and the 10^{-7} automotive benchmark TI reports for its ASIL-D-assessed wireless BMS [22]. At the operating points used in Section 3.2 (18 dB SNR under nominal EMI for both links, falling to 14 dB for NFC and 12 dB for BLE under aggressive EMI), nominal operation sits comfortably below the benchmark, while aggressive EMI pushes NFC to roughly 9.4×10^{-4} and BLE to roughly 1.8×10^{-4} - both above benchmark, and both regimes in which retransmissions dominate network behavior, as propagated into latency in Section 3.2.

3.2 Synchronization Latency and Network-Formation Scalability

For a network of N CMUs in which each node occupies a fixed slot t_slot, and each transmission is retried with probability p_fail on failure, expected network-formation time is

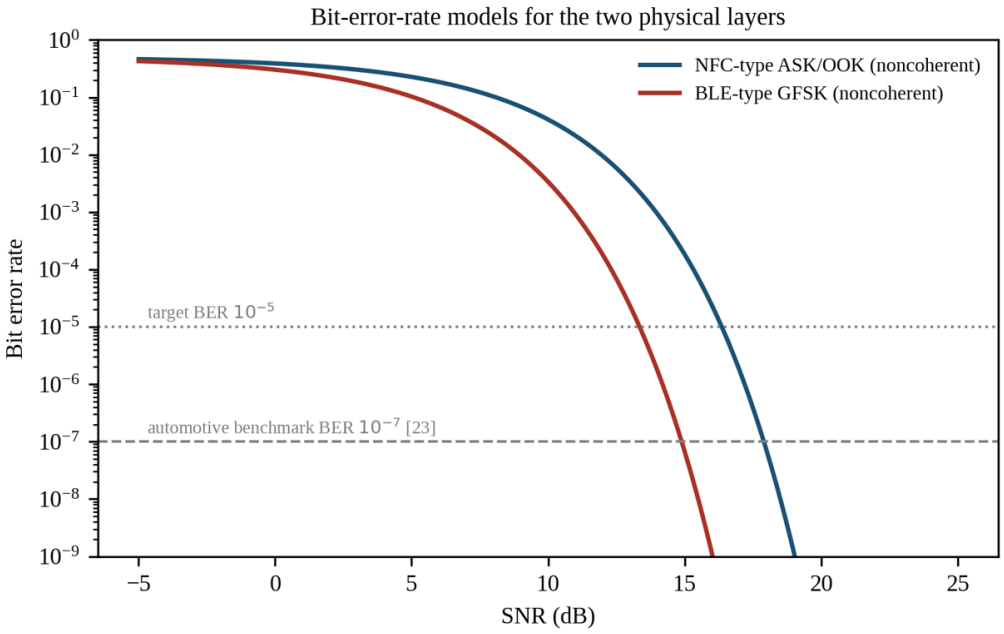


Figure 3: Bit-error-rate models for the ASK/OOK (NFC-type) and GFSK (BLE-type) physical layers, with automotive and telemetry BER thresholds.

$$T_form(N) = N \cdot t_slot/(1 - p_fail), p_fail = 1 - (1 - BER)^L \tag{3}$$

where L is packet length (128 bits, a short telemetry frame) and p_fail follows from the bit-error rates in Section 3.1. We set $t_slot = 2ms$ for the TDMA/BLE architecture, matching TI's reported per-node latency [22], and $t_slot = 22ms$ for sequential NFC polling, representative of ISO 15693-class anti-collision timing [23], [24].

Fig. 4 plots T_form against N from 8 to 96 CMUs for both architectures under both EMI scenarios; the eight-CMU point marks the configuration physically demonstrated in [1]. Two results stand out. First, the architectures scale on parallel linear trajectories roughly an order of magnitude apart: at $N = 96$, TDMA/BLE forms its network in under 0.2 s even under aggressive EMI, while sequential NFC polling — our own demonstrator's architecture — requires about 2.1˘2.4 s. Second, EMI-driven retransmission is a second-order effect here: aggressive EMI adds only about 13% to NFC formation time and 2% to BLE, since both links retain enough margin that most packets succeed on the first attempt. Practically, the demonstrator's polling architecture, adequate at eight CMUs **??**, would need a different medium-access scheme or parallelized readers to reach TI's sub-300 ms restart budget [22] at full pack scale.

3.3 Power-Budget Projection and Comparative Discussion

Because each retried transmission keeps a CMU's radio active longer than a successful exchange, retransmission also inflates pack-level current draw. We model this with a simple overhead term,

$$I_total(N) = N \cdot I_CMU \cdot (1 + k \cdot p_fail) \tag{4}$$

calibrated with $I_CMU = 0.09A$, measured in [1], and overhead coefficient $k = 0.35$. Fig. 5 shows the projection: at $N = 96$, nominal EMI draws approximately $8.64A$, close to ideal linear scaling, while aggressive EMI raises this to approximately $8.98A$ — a modest four-percent penalty rather than a runaway effect.

Table 1 draws these results together with the wider protocol landscape from Section 1.1, making the paper's central conclusion explicit: the TDMA/BLE branch - architecturally identical to GM's Ultium system [21] and TI's ASIL-D-assessed protocol [22] — is the only option combining adequate EMI

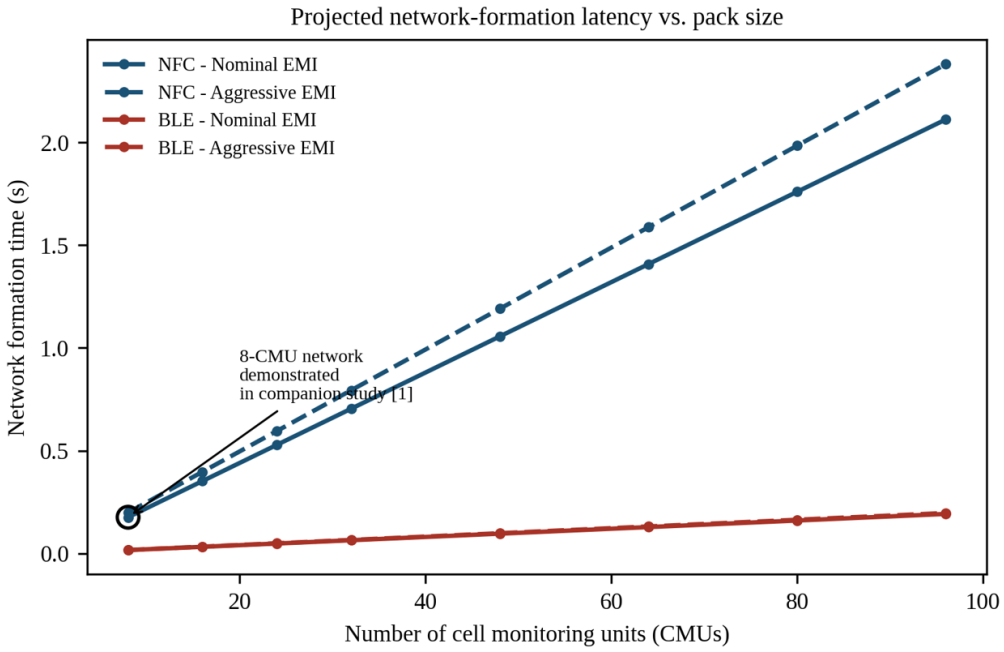


Figure 4: Projected network-formation latency vs. pack size for polling-based NFC and TDMA-based BLE architectures under nominal and aggressive EMI.

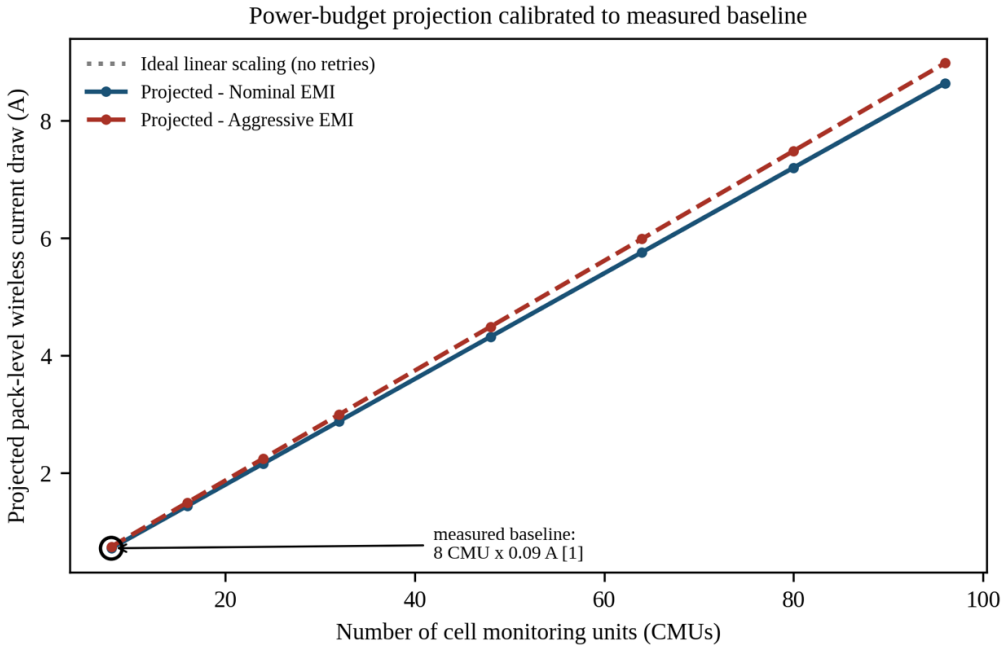


Figure 5: Projected pack-level wireless current draw vs. pack size, calibrated to the 0.09 A per-CMU base-line measured in the companion demonstrator.

Protocol	Data rate	Typical range	EMI robustness (this study / literature)	Sync. architecture	ASIL feasibility
Wi-Fi 6/7	10–40 Gbps	tens of m	Low — wide bandwidth increases exposure to switching harmonics	Contention-based (CSMA)	Not demonstrated
ZigBee (802.15.4)	250 kbps	10–100 m	Moderate — narrowband, but shares congested 2.4 GHz ISM band	Mesh / beacon	Not demonstrated
BLE	up to 2 Mbps	1–10 m (in-pack)	Moderate–High - FHSS/GFSK; ≈ 2% packet-failure penalty under aggressive EMI (this study)	TDMA (automotive variants)	ASIL-D assessed [23]
NFC/RFID (chip-on-cell)	≈ 26 – 53 *kbps*	<0.3 m (near field)	High below ≈ 10*cm*, degrades sharply beyond ≈ 13*cm* (this study)	Sequential anti-collision polling	Not yet ASIL-D assessed
UWB	> 100 Mbps	1–10 m	High - wide bandwidth, low PSD, resilient to narrowband EMI	TDMA / ranging-based	Not yet demonstrated

Table 1: Comparative summary of wireless physical layers for automotive cell-level monitoring, combining literature-reported properties with the quantitative results of Sections 3.1–3.3.

margin, sub-decisecond formation latency at full scale, and a documented path to ASIL-D certification via a black-channel safety layer [19], [20], [22]. The chip-on-cell NFC approach validated in [1] remains attractive where short range is an asset: tight coupling gives inherent security-through-proximity that a 2.4 GHz link must instead achieve through cryptography [9]. But its sequential-polling architecture needs parallel readers or a hybrid TDMA handover before meeting automotive restart budgets at production scale. Both branches benefit from the same quantified guidance: near-field coupling distance below roughly ten centimetres, and BLE enclosure attenuation/frequency-hopping margin sufficient to absorb a ten-to-twenty-decibel noise-floor rise without crossing the automotive BER benchmark [22].

4 Conclusion

This paper extended a previously reported, experimentally validated chip-on-cell wireless BMS demonstrator [1] into a calibrated analytical study of the two barriers most consistently flagged, but least often quantified, in the wBMS literature: EMI robustness and network-synchronization scalability. From a near-field/far-field link-budget model we derived bit-error-rate behavior for NFC and BLE under nominal and aggressive automotive EMI, propagated it through a discrete time-slot synchroniza-tion model to project network-formation latency from eight to ninety-six CMUs, and calibrated a power-budget projection against the demonstrator's measured 0.09 A per-CMU draw.

Three findings carry direct design relevance. Near-field NFC coupling loses margin roughly three times faster with distance than far-field BLE, quantitatively confirming the antenna-placement caution our companion study could previously only state qualitatively [1]. Medium-access architecture, not EMI severity, dominates synchronization scalability: TDMA/BLE forms a ninety-six-node network roughly an order of magnitude faster than sequential polling, regardless of EMI scenario. And electromagnetic aggression is, within the modeled range, a second-order effect once adequate nominal margin and frequency-hopping are present — reassuring, but not a license to relax the shielding and placement assumptions of Section 3.1.

The results indicate that the chip-on-cell NFC architecture is well suited to modules where simplicity and proximity security are priorities, but that automotive-grade, ASIL-D-relevant restart budgets at full-pack scale currently favor a TDMA/BLE-class architecture of the kind fielded by General

Motors [21] and safety-assessed by Texas Instruments [22]. We recommend, for teams extending demonstrators like [1] toward production intent: budgeting near-field coupling distance conservatively below ten centimetres; treating the wireless link as a black channel wrapped in an independent safety layer rather than qualifying the radio link itself to ASIL-D [19], [20]; and sizing frequency-hopping margin against a twenty-decibel, not merely nominal, noise-floor rise. This study is analytical, and its results are only as good as the parameters used to calibrate them; each assumption is stated explicitly and sourced to the demonstrator or to published literature, so the model can be re-calibrated as harder data arrives.

The natural next step is to feed real electromagnetic-chamber measurements from the SPI+BMC hardware in [1] back into these models, and to extend the synchronization framework to incorporate the cybersecurity threat classes catalogued by Murlidharan et al. [9], since an attacker inducing retransmissions and an inverter doing so incidentally place similar demands on the same synchronization budget.

References

[1] A. Simo, S. Dzitac, L. Ferestyan, I. Pandelica, C.-D. Dumitru, and A. Gligor, Performance Assessment of Wireless Architectures for Automotive Battery Management Systems, companion study, in preparation, 2026.

[2] Z. Cao, W. Gao, Y. Fu, and C. Mi, Wireless Battery Management Systems: Innovations, Challenges, and Future Perspectives, *Energies*, vol. 17, no. 14, p. 3277, Jul. 2024.

[3] A. Samanta and S. S. Williamson, A Survey of Wireless Battery Management System: Topology, *Emerging Trends, and Challenges, Electronics*, vol. 10, no. 2193, 2021.

[4] S.-J. Na, J.-U. Sim, B.-J. Kim, and I.-H. Cho, Design of Bluetooth Communication-Based Wireless Battery Management System for Electric Vehicles, *IEEE Access*, vol. 12, pp. 185946–185957, 2024.

[5] F. Basic, M. Gaertner, and C. Steger, Secure and Trustworthy NFC-based Sensor Readout for Battery Packs in Battery Management Systems, arXiv preprint arXiv:2310.10653, Aug. 2023; and F. Basic, C. R. Laube, P. Stratznig, C. Steger, and R. Kofler, Wireless BMS Architecture for Secure Readout in Vehicle and Second Life Applications, arXiv preprint arXiv:2311.12345, Nov. 2023.

[6] C. Shell, J. Henderson, H. Verra, and J. Dyer, Implementation of a Wireless Battery Management System (WBMS), in *Proc. IEEE I2MTC*, Pisa, Italy, 2015.

[7] M. Lee, S. Park, and J. Kim, Wireless Battery Management System, in *Proc. EVS27 Int. Battery, Hybrid and Fuel Cell Electric Vehicle Symposium*, Barcelona, Spain, 2013.

[8] H. A. Gabbar, A. M. Othman, and M. R. Abdussami, Review of Battery Management Systems (BMS) Development and Industrial Standards, *Technologies*, vol. 9, no. 2, p. 28, 2021.

[9] V. R. Murlidharan, J. Karnati, and H. Malik, BMS Threat Modeling, Vulnerability Analysis, and Cybersecurity Strategy, *IEEE Access*, vol. 13, pp. 144322–144336, 2025.

[10] D. Ghazali, N. A. A. Aziz, and M. K. Hassan, Advanced Algorithms in Battery Management Systems for Electric Vehicles: A Comprehensive Review, *Symmetry*, vol. 17, no. 1, p. 111, 2025.

[11] S. Kumar, An Efficient Battery Management System for Electric Vehicles, *Energy Conversion and Management*, vol. 295, p. 117495, 2025.

[12] S. Mulpuri, B. Sah, and P. Kumar, An Intelligent Battery Management System with End–Edge–Cloud Connectivity, *Energy & Environmental Science*, vol. 18, pp. 1302–1316, 2025.

[13] Z. Ren, H. Zhao, S. Chen, and T. Wang, Design and Implementation of a Battery Management System with Active Charge Balance, *Energy*, vol. 166, pp. 637–648, 2019.

[14] M. Balasingam, M. Ahmed, and K. Pattipati, Battery Management Systems — Challenges and Some Solutions, *Energies*, vol. 13, no. 9, p. 2142, 2020.

[15] M. Lelie, S. Braun, J. Ringbeck, K. Rumpf, and D. U. Sauer, Battery Management System Hardware Concepts: An Overview, *Applied Sciences*, vol. 8, no. 4, p. 534, 2018.

[16] S. Riurean and C. Rus, Optical Wireless Battery Management System for Enhanced Performance and Safety, in *Digital Technology Platforms and Deployment*, T. Antipova, Ed., Information Systems Engineering and Management, vol. 36, Springer, Cham, 2025, pp. 309–321.

[17] S. Je Lee, Y. H. Lee, J. Park, and N. Park, Analyzing RF Interference on Wireless BMS in High-Congestion Environments, in *Proc. IEEE Green Energy and Smart Systems Conference (IGESSC)*, Long Beach, CA, USA, 2023.

[18] S. Prüfling, T. Steffenhagen, O. Kazanci, et al., Elektronikdesign und funktionale Sicherheit bei drahtlosen Batteriemanagementsystemen, *ATZ – Automobiltechnische Zeitschrift*, vol. 126, pp. 42–47, 2024.

[19] P. C. John and B. P. N. Kumar, Functional Safety Design and ISO 26262 Compliance for BMS in EV and HEV, in *Intelligent Solutions for Smart Grids and Smart Cities*, P. Siano, S. Williamson, and S. Beevi, Eds., Springer, Singapore, 2023, pp. 329–339.

[20] ISO 26262:2018, Road Vehicles — Functional Safety, 2nd ed., International Organization for Standardization, Geneva, Switzerland, 2018.

[21] S. Cherry, GM Can Manage an EV's Batteries Wirelessly — and Remotely, *IEEE Spectrum*, Jun. 2021.

[22] Texas Instruments, The Next Generation Wireless BMS Using the CC2662R-Q1, Technical presentation SLYP857, Texas Instruments, Dallas, TX, 2023.

[23] K. Finkenzeller, RFID Handbook: Fundamentals and Applications in Contactless Smart Cards, Radio Frequency Identification and Near-Field Communication, 3rd ed., Wiley, Chichester, U.K., 2010.

[24] ISO/IEC 15693-3:2019, Cards and Security Devices for Personal Identification — Contactless Vicinity Objects, International Organization for Standardization, Geneva, Switzerland, 2019.

[25] J. G. Proakis and M. Salehi, Digital Communications, 5th ed., McGraw-Hill, New York, NY, 2008.

[26] CISPR 25:2021, Vehicles, Boats and Internal Combustion Engines — Radio Disturbance Characteristics — Limits and Methods of Measurement for the Protection of On-Board Re-ceivers, IEC, Geneva, Switzerland, 2021.



Copyright ©2026 by the authors. Licensee Agora University, Oradea, Romania.
This is an open access article distributed under the terms and conditions of the Creative Commons Attribution-NonCommercial 4.0 International License.
Journal's webpage: http://univagora.ro/jour/index.php/ijccc/



This journal is a member of, and subscribes to the principles of,
the Committee on Publication Ethics (COPE).
https://publicationethics.org/members/international-journal-computers-communications-and-control

Cite this paper as:

Simo, A.; Dzitac, S.; Neagu, B.-C.; Oros, H. (2026). Electromagnetic Interference Robustness and Synchro-nization Scalability in Wireless Battery Management Systems for Electric Vehicles, *International Journal of Computers Communications & Control*, 21(6), 7750, 2026.
https://doi.org/10.15837/ijccc.2026.6.7750